

## RESEARCH ARTICLE

# Strike mechanics of an ambush predator: the spearing mantis shrimp

M. S. deVries<sup>1,\*</sup>, E. A. K. Murphy<sup>2</sup> and S. N. Patek<sup>2</sup>

<sup>1</sup>Department of Integrative Biology, University of California, Berkeley, CA 94720, USA and <sup>2</sup>Department of Biology, Organismic and Evolutionary Graduate Program, University of Massachusetts, Amherst, MA 01003, USA

\*Author for correspondence (msdevries@berkeley.edu)

### SUMMARY

**Ambush predation is characterized by an animal scanning the environment from a concealed position and then rapidly executing a surprise attack. Mantis shrimp (Stomatopoda) consist of both ambush predators ('speakers') and foragers ('smashers'). Speakers hide in sandy burrows and capture evasive prey, whereas smashers search for prey away from their burrows and typically hammer hard-shelled, sedentary prey. Here, we examined the kinematics, morphology and field behavior of spearing mantis shrimp and compared them with previously studied smashers. Using two species with dramatically different adult sizes, we found that strikes produced by the diminutive species, *Alachosquilla vicina*, were faster (mean peak speed  $5.72 \pm 0.91 \text{ ms}^{-1}$ ; mean duration  $3.26 \pm 0.41 \text{ ms}$ ) than the strikes produced by the large species, *Lysiosquillina maculata* (mean peak speed  $2.30 \pm 0.85 \text{ ms}^{-1}$ ; mean duration  $24.98 \pm 9.68 \text{ ms}$ ). Micro-computed tomography and dissections showed that both species have the spring and latch structures that are used in other species for producing a spring-loaded strike; however, kinematic analyses indicated that only *A. vicina* consistently engages the elastic mechanism. In the field, *L. maculata* ambushed evasive prey primarily at night while hidden in burrows, striking with both long and short durations compared with laboratory videos. We expected ambush predators to strike with very high speeds, yet instead we found that these spearing mantis shrimp struck more slowly and with longer durations than smashers. Nonetheless, the strikes of speakers occurred at similar speeds and durations to those of other aquatic predators of evasive prey. Although counterintuitive, these findings suggest that ambush predators do not actually need to produce extremely high speeds, and that the very fastest predators are using speed to achieve other mechanical feats, such as producing large impact forces.**

Supplementary material available online at <http://jeb.biologists.org/cgi/content/full/215/24/4374/DC1>

Key words: foraging, raptorial appendage, Stomatopoda, Crustacea, kinematics, morphology, sit-and-wait predator.

Received 31 May 2012; Accepted 10 September 2012

### INTRODUCTION

Ambush predators minimize the distance between themselves and their prey over short time scales (Pianka, 1966; Huey et al., 1984; Webb, 1984; Garland and Losos, 1994; Miles et al., 2007; McBrayer and Wylie, 2009). The predator must avoid detection (Bailey, 1986; Kral et al., 2000; Bilcke et al., 2006; Eskew et al., 2009), attain high accelerations and speeds (Cooper et al., 1985; Alfaro, 2002; reviewed in McBrayer and Wylie, 2009), and retain some control over strike kinematics (van Leeuwen et al., 2000; Deban et al., 2001). To achieve these goals, ambush predators use three strategies to capture prey: (1) concealment through burrows or camouflage, (2) quick traverse of a potentially large distance to prey and (3) rapid attack to impact prey before escape. These strategies enable ambush predators to capture highly mobile prey that move within their striking distance, as opposed to foraging for sedentary prey, which are often consumed by widely foraging predators (Huey and Pianka, 1981; Greef and Whiting, 2000; Scharf et al., 2006). The morphological and kinematic strategies of ambush predators have been well studied in terrestrial animals, including the burst locomotion of lizards (Casatti and Castro, 2006; Miles et al., 2007; McBrayer and Wylie, 2009), the protrusible tongues of frogs (reviewed in van Leeuwen et al., 2000), the prey-capture appendages of the praying mantis (Corrette, 1990), and web building in spiders to facilitate ambush predation (Riechert

and Luczak, 1982), but few studies have examined ambush predation in aquatic systems. Here, we addressed basic questions about the mechanics, scaling and variation of aquatic ambush strikes in mantis shrimp (Stomatopoda).

In an aquatic environment, ambush predators must overcome challenges imposed by the density and viscosity of water. Some ambush predators, including snakes, fish and insects (Daniels, 1982; Cooper et al., 1985; Bailey, 1986; Formanowicz and Brodie, 1988; Alfaro, 2002; Bilcke et al., 2006; Hulbert et al., 2006; Ostrand et al., 2004; Sano and Kurokura, 2011) orient their bodies toward the prey so that they can strike quickly and accurately, while also minimizing disturbance to the water around them. Alternatively, some ambush predators, such as copepods that sit motionlessly in the water column to prevent detection by the prey (Kiørboe et al., 2010), are known to locate prey using hydrodynamic cues, which they then exploit to precisely time attacks (Jiang and Poffenbörger, 2008). Upon striking, aquatic ambush predators must effectively manipulate their strikes so as not to push water, and therefore the prey, out of the range of attack. The garter snake, *Thamnophis rufipunctatus*, ambushes prey from a hiding place by producing a rapid scissor strike that may drive water into the mouth and increase the chances of capturing prey (Alfaro, 2002). The wrasse, *Serranus cabrilla*, which uses the power of suction feeding to capture evasive fish prey, produces higher flow velocities in the buccal cavity

compared with the widely foraging species *Serranus scriba*, when the two species are given the same prey items (Viladiu et al., 1999).

Spearing mantis shrimp, hereafter ‘spearkers’, are another group of ambush predators that use elongate, streamlined appendages to ambush soft-bodied, evasive fish and crustaceans (Caldwell and Dingle, 1975) (Fig. 1). In contrast, ‘smasher’ mantis shrimp use hammer-shaped appendages to smash hard-shelled mollusks and crustaceans (Caldwell and Dingle, 1975; Caldwell and Dingle, 1976; Dingle and Caldwell, 1978) with strikes that can reach speeds of 14–23 ms<sup>-1</sup> (Patek et al., 2004; Patek et al., 2007). To our knowledge, no studies to date have recorded the strike kinematics of spearkers, although they constitute the majority of this 400+ species clade (Ahyong, 2001; Porter et al., 2010).

To achieve fast strikes, mantis shrimp rely on a network of structures that enhance the rate of movement beyond what could be generated by muscle alone. Together, these structures constitute a power amplification system (Fig. 1) (Burrows, 1969; Patek et al., 2004; Patek et al., 2007; Claverie et al., 2011; Patek et al., 2011). Preparation for the strike begins with simultaneous contractions of extensor and flexor muscles in the merus (McNeill et al., 1972). Extensor muscles proximally rotate an elastic spring (the ‘meral-V’) and lever system, while compressing a secondary elastic, saddle-shaped structure (the ‘saddle’) (Patek et al., 2004; Patek et al., 2007; Zack et al., 2009). At the same time, flexor muscles engage a pair of sclerites that act as a latch to prevent the propodus from rotating forward (Burrows, 1969; Burrows and Hoyle, 1972;

McNeill et al., 1972; Patek et al., 2007). When the sclerites are released, the carpus rotates and causes the propodus to slide along the merus. The propodus and dactyl then suddenly transition from sliding to rotating outward toward the prey. Both smashers and spearkers have the requisite structures for generating spring-loaded strikes (Burrows, 1969); however, it is not known whether or how spearkers use the power amplification system.

Here, we addressed three general questions about the kinematics and morphology of ambush predation. We examined these questions in two species of spearing mantis shrimp, *Lysiosquillina maculata* and *Alachosquilla vicina*, that differ more than tenfold in body size, yet live in similar habitats where they perform ambush predation from their sandy burrows (Fig. 1) (Caldwell, 1991). We asked first, what are the key kinematic and mechanical differences between ambush predators of dramatically different sizes? Second, do ambush predators perform differently in the laboratory and field? Third, how does ambush predation vary across aquatic taxa and do these differences represent trade-offs among prey-capture strategies? We expected large and small spearkers to have similar strike mechanics, but the large species was expected to produce greater kinematic output given its large appendages or ‘out-levers’. Strike performance in the laboratory and field was not expected to differ and animals in the field were expected to spend a substantial amount of time scanning for prey. Although smashers produce fast strikes, large and small spearkers were expected to strike even more quickly, because spearkers must produce fast strikes in order to capture evasive prey, while smashers consume slow-moving, hard-shelled prey.

## MATERIALS AND METHODS

### Animal acquisition and care

Ten *L. maculata* (Fabricius 1793) (Crustacea: Stomatopoda: Lysiosquillidae) and five *A. vicina* (Nobili 1904) (Crustacea: Stomatopoda: Nannosquillidae) specimens were collected at Lizard Island, Australia (Permits PRM01599G and G07/23055.1) or purchased from local aquarium stores. *Lysiosquillina maculata* body size, measured from rostrum to telson, ranged from 130 to 170 mm. *Alachosquilla vicina* body size ranged from 24 to 27 mm. Animals were maintained at 25°C, in 34–36 p.p.t. artificial seawater. *Lysiosquillina maculata* were kept in individual recirculating tanks (32 cm height×52 cm width×26 cm depth), whereas *A. vicina* individuals were kept communally in a standard 371 aquarium. Animals built their own burrows in fine sediment (20–27 cm depth for *L. maculata* and ~5 cm depth for *A. vicina*; sugar-sized Oolite, Aragonite, CaribSea, White City, FL, USA). *Lysiosquillina maculata* were fed frozen and freeze-dried shrimp twice weekly and *A. vicina* were fed live or frozen brine shrimp 2–3 times weekly.

### Appendage morphology

Dissections and micro-computed tomography (micro-CT) were used to reconstruct the morphology of the raptorial appendage. Freshly frozen *L. maculata* and *A. vicina* specimens were scanned by the High-Resolution X-ray Computed Tomography Facility (ACTIS, Bio-Imaging Research Inc.) at the University of Texas, Austin (slice thickness 0.1078 mm, resolution 1024×1024 pixels), and the Center for Nanoscale Systems at Harvard University (Model HMXST225, X-Tek, Nikon Metrology NV, Leuven, Belgium) (slice thickness 0.0057 mm, resolution 2000×2000 pixels), respectively. Surface volume rendering (Phong algorithm) and mineralization patterns (sum along ray algorithm) were used to visualize the component structures of each raptorial appendage (VGStudio Max v. 2.0, Heidelberg, Germany).

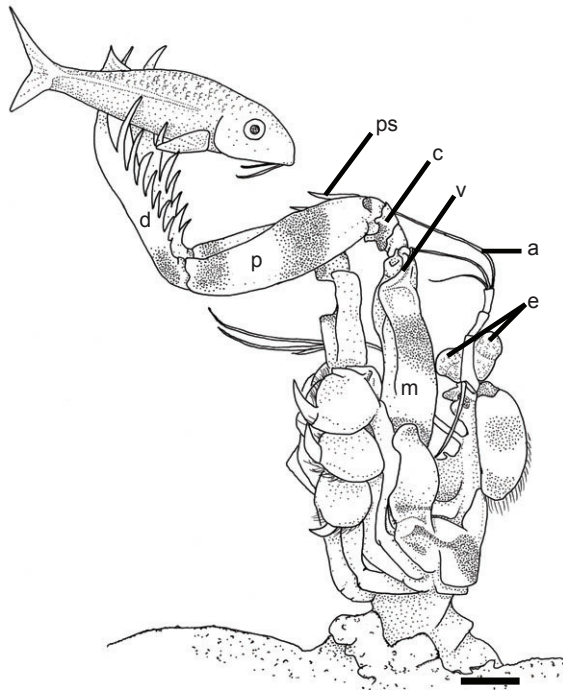


Fig. 1. *Lysiosquillina maculata* is depicted rapidly emerging from its sandy burrow to capture a fish with the two most distal spines of the dactyl. *Alachosquilla vicina* (not shown) employs similar predatory behavior while catching smaller evasive prey. Structures labeled on the lateral side of the left raptorial appendage highlight the primary anatomical features involved in prey capture. The individual is positioned vertically with half of its body exposed so that dorsal is oriented to the right of the page and ventral is oriented to the left. Labeled structures, listed from the distal to proximal end of the individual, are: dactyl (d), propodus (p), moveable propodal spine (ps), carpus (c), meral-V (v), merus (m), antennule (a), eyes (e). Scale bar, 10 mm.

### High-speed videography of strike kinematics

Strikes were elicited by presenting prey to the study animals. *Lysiosquillina maculata* individuals were presented with tethered frozen shrimp that were actively moved away from the stomatopods by hand when stomatopods would strike, to mimic evasive prey. *Alachosquilla vicina* individuals were presented with live brine shrimp released from a pipette. Raptorial strikes were filmed laterally at 3000 frames s<sup>-1</sup> for *L. maculata* (0.2 ms shutter duration, 1024×1024 pixel resolution) and at 10,000 frames s<sup>-1</sup> for *A. vicina* (0.04 ms shutter duration, 512×512 pixel resolution) using a digital high speed imaging system (APX-RS, Photron USA Inc., San Diego, CA, USA).

### Digital image analysis

For *L. maculata*, four landmarks were tracked on each video frame, beginning at the onset of dactyl rotation and ending when propodus rotation ceased (Matlab v. R2006a–R2008b, The Mathworks, Natick, MA, USA). Displacement of the propodus and dactyl was measured from three landmarks: the anterior–distal tip of the carpus, the distal trailing edge of the propodus, and the tip of the distal, leading edge of the dactyl (Fig. 2A, points 2–4; for definitions of anatomy, refer to Fig. 1). To determine the amount of appendage movement that was not due to propodus and dactyl rotation alone, merus movement was measured from the distal tip of the meral-V (Fig. 2A, point 1). All video sequences were digitized 2–5 times and the mean pixel location of each landmark was calculated for each frame. Points were digitized only if they were visible in all frames for the duration of the strike. Measurement error was estimated by digitizing five sequences 3–5 times; the percentage error averaged 5±4% for each point (range 0–7%).

For *A. vicina*, the movement of each appendage segment was tracked starting when carpus rotation began and ending when propodus rotation stopped. Lines were drawn from the proximal to distal end of each appendage segment and points were digitized at the intersections or end of each line (Fig. 2B). Propodus displacements were measured using the distal end of the propodus (Fig. 2B, point 4) following the methods for *L. maculata*. Displacement of the distal end of the merus (Fig. 2B, point 2) was digitized and then subtracted from propodus displacement to ensure that merus movement did not influence propodus kinematics (Matlab v. R2006a–R2008b, The Mathworks). Digitizing error was calculated by digitizing one strike sequence 10 times and then analyzing the difference in *x*- and *y*-coordinates at the distal and proximal end of each segment (Fig. 2B). The average percentage error was 0.12±0.02% (range 0.00–4.21%). At the beginning and end of the strike, digitizing error was often greater than propodus displacement; therefore, if the displacement was less than 0.2 mm

at any frame in the first 15% or last 10% of the strike's duration, then that frame and all previous or subsequent frames, respectively, were removed from kinematic analysis.

Some strikes were off-axis relative to the camera's plane of view. For *L. maculata*, the lateral side of each appendage segment was photographed (D70 digital SLR camera, Nikon Corporation, Tokyo Japan) and measured (Matlab v. R2006a–R2008b, The Mathworks). The cosine of the length measured from the videos was divided by the known length measured from the appendage segments to determine the angle of the segments relative to the camera. We then divided the displacement measured from the videos by the cosine of the off-axis correction angle, the result of which equaled the actual displacement. *Alachosquilla vicina* strikes were used only if they were in focus for the duration of the strike; the camera lens was kept at a constant distance (29.8 cm) from each focal burrow. To calculate the maximum displacement error, we measured the focal depth by calculating the closest and furthest point at which a ruler was in focus.

### Strike kinematics

For *L. maculata*, speed and acceleration of the distal ends of the merus, propodus and dactyl were calculated separately and relative to the movement of the other appendage segments (25 sequences, 5 individuals, 3–8 sequences per individual). For example, propodus speed was calculated relative to merus movement. First, cumulative linear and angular displacements between video frames were measured. Angular displacement of the propodus about the propodus–carpus joint was measured by using propodus displacement as the arc length and then dividing this arc length by propodus length (i.e. the radius), yielding the change in angle between frames. Displacement of the appendage segments was processed using three curve-fitting methods: 200 Hz Butterworth filter, 10th order polynomial curve fit, and an interpolated spline (Fig. 3) (Walker, 1998) (Matlab v. R2006a–R2008b, The Mathworks). A 10th order polynomial provided the best curve-fitting performance for displacement (Fig. 3), because it best minimized the amplitude of the residuals along the length of the curve. Speed and acceleration were calculated as the first and second derivatives of the curve-fit cumulative displacement data.

For *A. vicina*, speed (27 strikes, 5 individuals, 1–12 strikes per individual) and acceleration (12 strikes, 4 individuals, 1–4 strikes per individual) of the propodus were calculated. Angular speed of the propodus was also calculated by dividing displacement (arc length) by propodus length (the radius). *Alachosquilla vicina* strikes often yielded too few video frames for a 10th order polynomial to accurately smooth the data. Thus, for 19 or fewer frames, we used a 4th order polynomial and for 20 or more frames, we used a 10th order polynomial. Speed and acceleration were calculated by taking

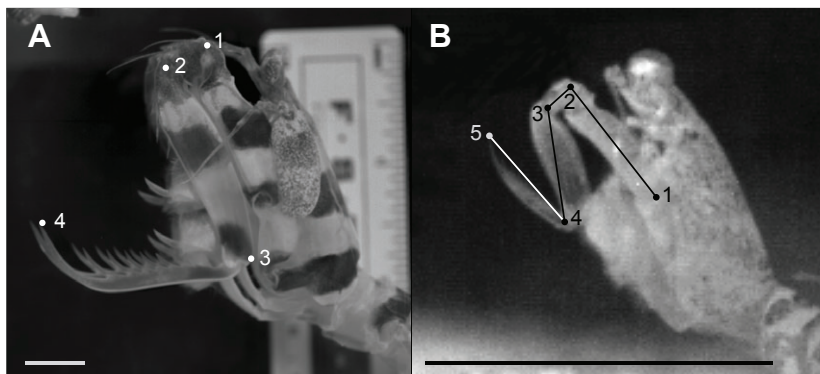


Fig. 2. High speed video images of *L. maculata* and *A. vicina* in lateral view overlaid with the digitized points. (A) *Lysiosquillina maculata*. Numbers represent anatomical locations of the points: (1) the tip of the distal edge of the meral-V, (2) the anterior–distal edge of the carpus, (3) the distal, trailing edge of the propodus, and (4) the tip of the dactyl. (B) *Alachosquilla vicina*. The digitized points are located at: (1) the ischium–merus joint, (2) the merus–carpus joint, (3) the carpus–propodus joint, (4) the propodus–dactyl joint, and (5) the tip of the dactyl. Scale bars, 10 mm.

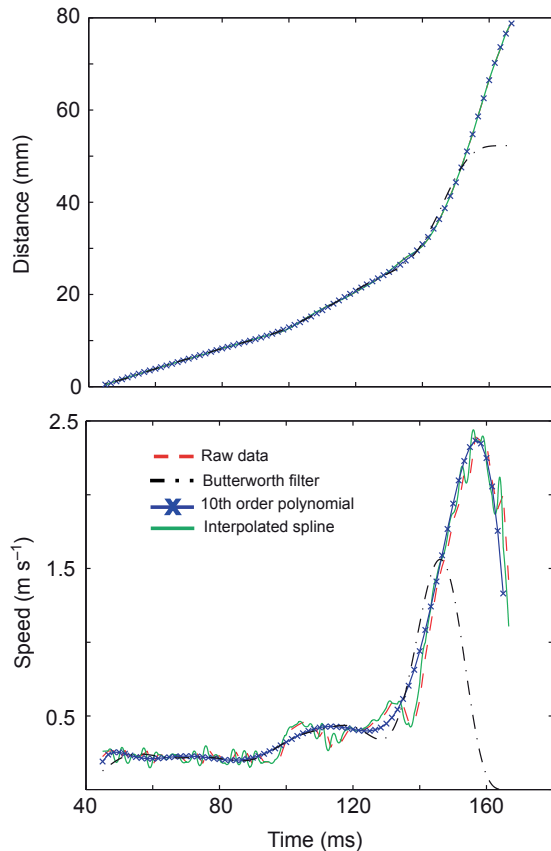


Fig. 3. A typical *L. maculata* strike showing dactyl movement over time. Distance and speed (red lines, upper and lower graphs, respectively) were filtered with a Butterworth filter (black lines), fitted with an interpolated spline (green lines), and fitted with a 10th order polynomial curve fit (blue lines). The 10th order polynomial yielded the best curve fit.

the first and second derivatives of the curve-fit cumulative displacement data. The parts of the strike for which all points were visible were digitized. If maximum acceleration occurred at the very beginning or end of the digitized portion of a strike, the high acceleration could have resulted from deceleration prior to the start of the video or acceleration afterwards; therefore, it was ambiguous whether we measured maximal acceleration in those particular strikes. Those strike sequences were thus removed from the dataset.

For both species, we recorded the duration of propodus rotation when the appendage rotated to full extension, defined as the point at which the propodus reached an angle of 180 deg or greater relative to the merus (*L. maculata*: 40 sequences, 5 individuals, 6–15 strikes per individual; *A. vicina*: 59 strikes, 5 individuals, 5–35 strikes per individual). If maximum extension was reached by both appendages during a single strike, each appendage was analyzed and counted independently.

#### Evidence of spring loading

Given the contribution of the saddle, meral-V and meral sclerites (the ‘latch’) to strike kinematics in other mantis shrimp species (Burrows, 1969; Patek et al., 2007; Zack et al., 2009), we calculated the percentage of sequences in which the extension of the saddle and meral-V was visible. We also noted whether the carpus rotated and the propodus slid linearly along the merus prior to propodus rotation, because these movements probably indicate latch release (Burrows, 1969; Patek et al., 2004). The meral-V was visible in the

*L. maculata* videos; therefore, we were able to measure the displacement and rotation of the meral-V (16 sequences, 5 individuals, 3–4 strikes per individual). To determine the minimum resolution of the meral-V movement, we calculated the standard deviations of each point’s *x*- and *y*-coordinates, which ranged from 0.10 to 0.25 mm or from ~1 to 3 pixels. *Alachosquilla vicina*’s meral-V was too small to see in the high speed images and so we relied on saddle extension and the propodus sliding along the merus as evidence of spring loading.

#### Statistics

Peak speeds and accelerations of the propodus were determined for each video sequence for both species. The results are presented as means  $\pm$  1 s.d.

Within each species, we tested whether there were significant differences in strike speed and duration of propodus rotation between individuals (ANOVA: R v. 2.7.1, The R Foundation for Statistical Computing, Vienna, Austria). We then examined the relationship between body size and propodus speed in *L. maculata* by testing whether carapace length was correlated with the mean peak propodus speed (least-squares linear regression: R v. 2.7.1, The R Foundation for Statistical Computing; JMP v. 7.0, SAS Institute Inc., Cary, NC, USA).

We also tested whether the distance between an individual and its prey was correlated with strike speed and duration for both species. At the onset of dactyl rotation for *L. maculata* and at the onset of carpus rotation for *A. vicina*, we measured the distance between the center of the prey and the center edge of the mantis shrimp’s eye that was closest to the prey (Matlab v. R2008a–R2008b, The Mathworks). This distance was then divided by propodus length to account for body size differences between individuals. Propodus length was used because we were unable to remove *A. vicina* individuals from their burrows in order to take body size measurements. However, we confirmed that propodus length is highly correlated to body size in *L. maculata* (linear regression:  $R^2=0.77$ ,  $N=7$ ,  $F_{1,6}=21.51$ ,  $P<0.01$ ), which is consistent with the relationship between appendage components and body size in other mantis shrimp species (Dingle and Caldwell, 1978; Hamano and Matsuura, 1986; Patek and Caldwell, 2005; Claverie et al., 2011). Finally, we tested whether peak propodus speed was correlated with the size-corrected distance to the prey and whether individuals initiated strikes from significantly different distances (ANCOVA: R v. 2.7.1, The R Foundation for Statistical Computing; JMP v. 7.0, SAS Institute Inc.).

#### *Lysiosquillina maculata* field behavior

*Lysiosquillina maculata* activity was filmed at 17 burrows in the sand flats and mangroves of Lizard Island, Australia every day for 3 weeks in May 2009 (Permit no. G07/23354.1). Twelve burrows that were within 26 m of each other were filmed at Station Beach over 24 h periods (06:00h–08:30h, 2 burrows, each filmed for 2h; 09:00h–13:20h, 4 burrows, each filmed for 2–4h; 15:00h–18:00h, 2 burrows, each filmed for 2h; 17:00h–22:30h, 12 burrows, each filmed for 2–4h). Five burrows that were within 10 m of each other were filmed at Mangrove Beach from 11:20h to 14:30h (2 burrows, each filmed for 2h) and from 17:00h to 20:00h (3 burrows, each filmed for 2–4h). The majority of the recordings were at night at Station Beach (72h), because it became apparent early in the observations that this was when and where most feeding activity occurred. Note that while we recorded from unique burrows, it is possible (although unlikely) that burrows were connected below ground and individuals could have switched burrows during the experiments.

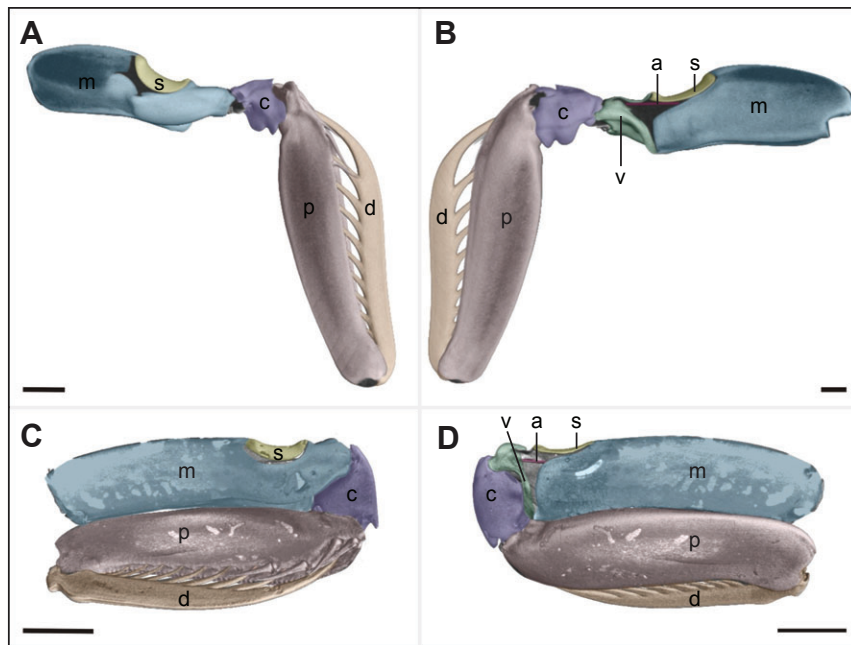


Fig. 4. Computed tomography (CT) images of *L. maculata* (A,B) and *A. vicina* (C,D) raptorial appendages. *Lysiosquilla maculata*'s propodus is open in the striking position whereas *A. vicina*'s propodus is pulled against the merus in the pre-strike position. The medial views (A,C) show the uniformly robust merus exoskeleton (m) whereas the lateral views (B,D) reveal the flexible saddle (s) and moveable meral-V (v) that are both part of the merus. The remaining anatomical features are labeled as follows: carpus (c), propodus (p), dactyl (d) and lateral extensor muscle apodeme (a). Scale bars, 1 mm. Note that the scale bars are different lengths because of the different sizes and orientations of the images relative to the plane of the page as calculated by the CT-processing software.

Feeding activity was filmed with two low-light underwater cameras (Submergible Submersible Under-Water CCD 480TVL Bullet Color Camera, Sony Corporation, NY, USA) connected to Hi-8 video recorders (30 frames  $s^{-1}$ , Sony GV-A500 Hi8 Video Walkman, Sony Corporation). One small dive light per camera was fitted with red filters and placed at  $\sim 45$  deg relative to the camera. The cameras were placed next to two different *L. maculata* burrows during each filming session and videos were later converted to digital format (ADVC55 Advanced Digital Video Converter, Grass Valley, Boulogne Cedex, France; iMovie, Apple Inc., CA, USA).

Strike durations were measured from the field videos by counting the number of frames over which the propodus and dactyl rotated forward (34 strikes, 7 burrows, 1–22 strikes per burrow). Behaviors associated with prey capture, such as lunges from the burrow and visual or olfactory scans for prey with the eyes or antennules were recorded. The presence of prey during these strikes was also noted.

## RESULTS

### Micro-CT scans

In both *L. maculata* and *A. vicina*, the propodus and dactyl exoskeletons are uniformly robust (Fig. 4). The saddles and meral-Vs are mineralized, and similarly shaped in the two species (Fig. 4). The apodemes of the lateral extensor muscles are apparent in the micro-CT scans (Fig. 4B,D).

### Strike kinematics

In both species, strikes began with the individual emerging from the burrow while the dactyl rotated distally relative to the propodus (Figs 5, 6). In *L. maculata*, the dactyl rotated with a mean linear speed of  $0.78 \pm 0.28 \text{ ms}^{-1}$  (range  $0.16$ – $1.41 \text{ ms}^{-1}$ ; Fig. 5). In *A. vicina*, the dactyl also moved slowly. For most *L. maculata* strikes and all *A. vicina* strikes, the carpus then rotated distally, causing the propodus to slide along the merus and then to rapidly swing away from the merus (Tables 1–3, Figs 5, 6; supplementary material Movies 1, 2). Peak instantaneous propodus linear speed ranged from  $0.91$  to  $4.52 \text{ ms}^{-1}$  in *L. maculata* (Table 1) and  $3.97$  to  $8.54 \text{ ms}^{-1}$  in *A. vicina* (Table 2). In *L. maculata*, peak speed occurred  $8.9$ – $24.6$  ms

after the onset of propodus rotation (Fig. 5). In *A. vicina*, peak speed occurred  $0.7$ – $1.5$  ms after the propodus began rotating (Fig. 6). The duration of propodus rotation ranged from  $20$  to  $67$  ms in *L. maculata* and  $1.9$  to  $4.5$  ms in *A. vicina* (Table 3).

### Evidence of spring loading

The carpus rotated and the propodus slid linearly along the merus in  $84 \pm 17\%$  of *L. maculata* strikes and in  $100\%$  of *A. vicina* strikes. The saddle compressed and extended in  $94 \pm 11\%$  of *A. vicina* strikes in which the saddle was visible. Specifically, the saddle remained compressed during carpus rotation, and then extended over two to three video frames as the propodus began to rotate outward (Fig. 6A1–A3). Saddle compression and extension did not occur in *L. maculata*. Movement of the meral-V in *L. maculata* was miniscule ( $0.5 \pm 0.32$  mm), and very close to the calculated movement resolution of  $\pm 3$  pixels, or  $0.25$  mm.

### Statistics

Carapace length of *L. maculata* was not correlated with peak propodus speed (least-squares linear regression:  $R^2=0.01$ ,  $N=5$ ,  $F_{1,23}=0.08$ ,  $P=0.78$ ). Differences in propodus speed (ANOVA:  $N=5$ ,  $F_{4,20}=1.03$ ,  $P=0.41$ ; Table 1) and strike duration (ANOVA:  $N=9$ ,  $F_{6,22}=2.42$ ,  $P=0.06$ ; Table 1) were also not significant between individual *L. maculata*.

The range of distances from which the animals initiated their strikes was small for *L. maculata* (prey were  $2$ – $5$  cm away at the start of dactyl rotation). There were no correlations between the size-corrected distance to the prey and linear and angular speed of either the propodus or the dactyl (ANCOVA: all  $P>0.05$ ; Fig. 7), nor were there significant correlations between distance to the prey and the duration of propodus movement (ANCOVA:  $N=9$ ,  $F_{7,21}=2.00$ ,  $P=0.1$ ). There was no effect of the individual on distance to the prey (ANOVA:  $N=9$ ,  $F_{6,22}=1.82$ ,  $P=0.14$ ).

*Alachosquilla vicina* individuals struck from a range of distances at freely swimming brine shrimp, shrimp partially emerged from the pipette, and the pipette itself (prey were  $4$ – $11$  mm away from the mantis shrimp at the start of propodus rotation) (supplementary material Movie 3). We examined whether propodus speed was

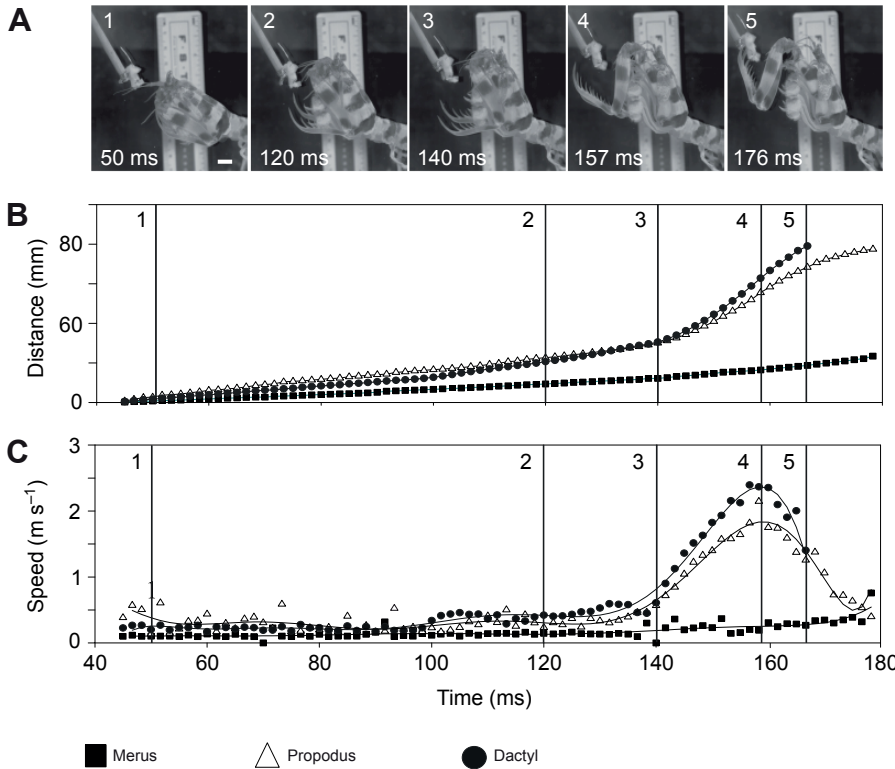


Fig. 5. A kinematic analysis with corresponding high speed images of a typical raptorial strike in *L. maculata*. (A) High speed images show (1) initiation of the strike with rotation of the dactyl away from the propodus, (2) completion of the propodus slide prior to propodus rotation, (3) full extension of the dactyl, (4) outward rotation of the propodus and (5) contact with the prey. (B) Cumulative displacement of the merus and distal ends of the propodus and dactyl. (C) Speed of the merus, propodus and dactyl. Solid lines represent the 10th order polynomial curve fits of the raw data. Numbers in B and C correspond to those in the high speed images in A. Scale bar, 10 mm.

affected by three factors: distance to the prey, individual, and the type of target (pipette, partially emerged brine shrimp or freely swimming brine shrimp). All three parameters examined together had no significant effect on propodus speed (two-way ANCOVA:  $N=5$ ,  $F_{16,10}=1.50$ ,  $P=0.26$ ). However, distance to the prey and individual had a significant effect on peak speed (one-way ANCOVA:  $N=5$ ,  $F_{8,18}=3.28$ ,  $P=0.02$ ; Fig. 7). There was also a significant effect of the object and individual on peak speed (two-way ANOVA:  $N=5$ ,  $F_{10,16}=2.94$ ,  $P=0.03$ ; Fig. 8). Finally, there were significant differences in speed between individuals (ANOVA:  $N=5$ ,  $F_{8,18}=3.28$ ,  $P=0.02$ ).

Duration of propodus rotation in *A. vicina* was significantly affected by all parameters examined: distance to prey, individual, and target (two-way ANCOVA:  $N=5$ ,  $F_{19,39}=3.70$ ,  $P<0.001$ ; Fig. 8). The distance to the prey was also affected by both the individual and target (two-way ANOVA:  $N=5$ ,  $F_{10,48}=8.11$ ,  $P<0.001$ ).

#### *Lysiosquillina maculata* field behavior

*Lysiosquillina maculata* behaved similarly in the laboratory and field. Prior to a strike, an individual's eyes were visible peeking out of the burrow entrance. Depending on the quality of the video, we could also see the antennules moving. Almost the entire body of

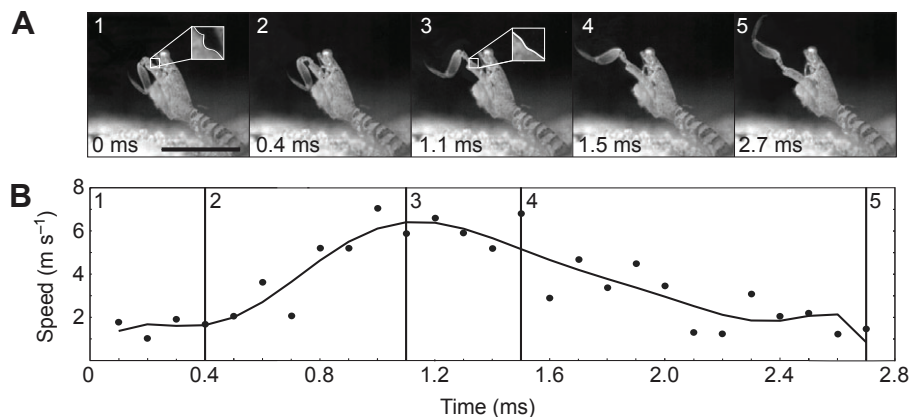


Fig. 6. A kinematic analysis of *A. vicina* striking at brine shrimp that actually evaded capture. (A) High speed images show propodus rotation during a right appendage strike (left appendage digitally removed for clarity). (1) The strike begins with the saddle compressed (inset; white line traced along dorsal surface) and the carpus and propodus positioned close to the merus. (2) While the saddle is still compressed, the propodus begins to slide distally without any rotation. (3) The saddle begins to extend (inset, white outline) as the propodus begins its outward rotation. (4,5) The saddle remains extended for the rest of the strike as the propodus fully extends toward the prey. (B) Speed of the distal end of the propodus. The numbers correspond with those in the high speed images in A. Speed is calculated from the derivative of the raw displacement data and from the derivative of the 10th order polynomial curve fit of the displacement data (black line). Scale bar, 10 mm.

Table 1. The kinematics of *L. maculata*'s strikes

| Individual                        | Speed (m s <sup>-1</sup> ) | Acceleration (m s <sup>-2</sup> ) | Angular speed (×10 <sup>3</sup> rad s <sup>-1</sup> ) | Angular acceleration (rad s <sup>-2</sup> ) | Duration (ms)     | Time of max. speed (ms) |
|-----------------------------------|----------------------------|-----------------------------------|---|---|-------------------|-------------------------|
| 1                                 | 2.00±0.90 (n=6)            | 0.40±0.69 (n=6)                   | 5.44±2.90 (n=6)                                       | 11.68±20.36 (n=6)                           | 28.56±6.15 (n=6)  | 15.39±5.70 (n=6)        |
| 2                                 | 1.94±0.37 (n=6)            | 0.13±0.04 (n=6)                   | 5.76±0.90 (n=6)                                       | 3.43±1.12 (n=6)                             | 49.27±15.39 (n=7) | 15.17±2.84 (n=6)        |
| 3                                 | 3.06±1.52 (n=3)            | 0.48±0.27 (n=3)                   | 8.33±4.12 (n=3)                                       | 13.81±7.85 (n=3)                            | 31.89±3.34 (n=15) | 12.78±6.26 (n=3)        |
| 4                                 | 2.36±0.87 (n=7)            | 0.21±0.25 (n=7)                   | 5.25±1.93 (n=7)                                       | 4.74±5.57 (n=7)                             | 36.5±10.32 (n=6)  | 24.57±9.40 (n=7)        |
| 5                                 | 2.14±0.60 (n=3)            | 0.26±0.26 (n=3)                   | 7.57±2.54 (n=3)                                       | 7.78±1.90 (n=3)                             | 24.0±5.7 (n=6)    | 8.89±2.55 (n=3)         |
| Mean of all<br><i>L. maculata</i> | 2.30±0.85 (N=5)            | 0.30±0.28 (N=5)                   | 6.47±2.48 (N=5)                                       | 4.43±7.77 (N=5)                             | 34.04±4.75 (N=5)  | 15.36±5.78 (N=5)        |

Acceleration and speed were measured at the distal end of the propodus. Time is the chronological location of maximum speed relative to the onset of propodus rotation. Duration is the amount of time between the onset of propodus rotation and full extension.

Values are means ± s.d. *n*, number of strikes for each individual; *N*, number of individuals.

the animal remained in the burrow for the majority of the videos, with only the eyes, antennules and antennule scales exposed. When the prey was within striking range of the burrow, the individual would lunge out of the burrow such that the abdominal segments were visible and then it would snare prey between the propodus and dactyl. In the majority of strikes (24 strikes from 3 burrows), both appendages struck the prey. All raptorial strikes occurred at Station Beach at night from 18:30 h to 21:00 h. In 24 strike sequences, individuals struck small, swimming prey.

When possible, we also calculated strike duration. Twenty-five strikes were confirmed predatory strikes, as characterized by an open dactyl during the strike. In 9 strikes, we were unable to discern whether the dactyl was open, because of low image resolution or the animal's orientation away from the camera. Nineteen strikes (7 burrows, 1–12 strikes per burrow) occurred within 1 video frame (≤33 ms) (see supplementary material Movie4) and 6 strikes (3 burrows, 1–3 strikes per burrow) occurred over 2 frames (≤66 ms).

## DISCUSSION

Although one might expect that predators capturing evasive prey would strike more quickly than predators gathering stationary prey, we found the opposite: both large and small spearing mantis shrimp struck surprisingly slowly compared with the 14–23 ms<sup>-1</sup> strikes recorded in smashers (Patek et al., 2004). Additionally, although one would expect larger animals to wield faster strikes as a result of their larger appendages, we were surprised to find that the largest spearers struck far more slowly than the smallest. We begin by comparing the kinematics and elastic mechanism of spearing strikes in the large species, *L. maculata*, and the small species, *A. vicina*, to shed light on why smaller spearers strike more quickly. We then compare spearers with other kinds of mantis shrimp as well as with the field behavior of other ambush and aquatic predators. We

conclude by considering how a collection of factors – strike reach, accuracy and duration – may influence strike kinematics and behavior in aquatic ambush predators.

### Kinematics and mechanics of small and large spearers

Even though *A. vicina* had appendages that were an order of magnitude smaller than those of *L. maculata*, *A. vicina* struck with far greater speed and acceleration. The linear speed of *A. vicina* strikes was nearly twice as fast those of *L. maculata*; angular speed as well as linear acceleration were at least one order of magnitude higher in *A. vicina* compared with *L. maculata*; and angular acceleration was several orders of magnitude higher in *A. vicina* compared with *L. maculata* (Table 3, Figs 9, 10). The interpretations of these findings are limited by the challenges of only comparing two species (Garland and Adolph, 1994); however, the differences in body size and appendage speed between these species raise interesting questions about interactions between kinematics and prey behavior at a variety of size scales.

In spite of their substantial size differences, the morphology of the segments and elastic structures were similar in the two species, as was evident in the CT-scans. However, these structures were not necessarily used in similar ways. *Alachosquilla vicina* appeared to perform spring-loaded strikes, given that the saddle extended during propodus rotation (Patek et al., 2007; Zack et al., 2009) and the propodus slid along the merus prior to forward rotation (Burrows, 1969). By contrast, the propodus slid along the merus in only some of *L. maculata*'s strikes but no movement of the elastic mechanism was visible: if the meral-V moved at all in the recorded strikes, then it moved at most 16% of the available space between the meral-V and merus.

As with all kinematic studies, it is important to consider whether maximal strike effort was elicited. The subtle differences in prey presentation – a shrimp that was manually moved away from *L.*

Table 2. The kinematics of *A. vicina*'s strikes

| Individual                      | Speed (m s <sup>-1</sup> ) | Acceleration (km s <sup>-2</sup> ) | Angular speed (×10 <sup>3</sup> rad s <sup>-1</sup> ) | Angular acceleration (×10 <sup>9</sup> rad s <sup>-2</sup> ) | Duration (ms)    | Time of max. speed (ms) |
|---------------------------------|----------------------------|------------------------------------|---|--|------------------|-------------------------|
| 1                               | 4.84±0.82 (n=6)            | 7.25±5.90 (n=4)                    | 1.41±0.37 (n=6)                                       | 2.06±1.86 (n=4)  | 3.76±0.45 (n=5)  | 1.02±0.2 (n=6)          |
| 2                               | 6.55±0.78 (n=12)           | 10.94±3.79 (n=4)                   | 2.15±0.22 (n=12)                                      | 3.57±1.07 (n=4)  | 2.76±0.41 (n=35) | 1.1±0.1 (n=12)          |
| 3                               | 5.71 (n=1)                 | n.d.                               | 1.49 (n=1)  | n.d.   | 3.41±0.50 (n=7)  | 1.1 (n=1)               |
| 4                               | 6.71±1.49 (n=5)            | 12.57±3.90 (n=3)                   | 1.73±0.44 (n=5)                                       | 3.29±1.05 (n=3)  | 2.9±0.59 (n=6)   | 1.3±0.14 (n=5)          |
| 5                               | 4.78±0.46 (n=3)            | 5.51 (n=1)                         | 1.28±0.03 (n=3)                                       | 1.37 (n=1)   | 3.45±0.62 (n=6)  | 0.8±0.1 (n=3)           |
| Mean of all<br><i>A. vicina</i> | 5.72±0.91 (N=5)            | 9.07±3.25 (N=5)                    | 1.61±0.34 (N=5)                                       | 2.58±1.04 (N=5)  | 3.26±0.41 (N=5)  | 1.1±0.2 (N=5)           |

Acceleration and speed were measured at the distal end of the propodus. Time is the chronological location of maximum speed relative to the onset of propodus rotation. Duration is the amount of time between the onset of propodus rotation and full extension.

Values are mean ± s.d. *n*, number of replicates for each individual; *N*, number of individuals; n.d., not determined.

Table 3. Comparison of mean *L. maculata* and *A. vicina* kinematic data

|                                | <i>L. maculata</i><br>(N=5–9) | <i>A. vicina</i><br>(N=5)                  | Differences between means<br>(species with higher value) |
|--------------------------------|-------------------------------|--|--|
| Peak speed                     |                               |  |  |
| Linear (m s <sup>-1</sup> )    | 2.30±0.85 (N=5)               | 5.72±0.91                                  | 3.42 ( <i>A. vicina</i> )                                |
| Angular (rad s <sup>-1</sup> ) | 64.72±24.76 (N=5)             | 1610±342                                   | 1545 ( <i>A. vicina</i> )                                |
| Peak acceleration              |                               |  |  |
| Linear (m s <sup>-2</sup> )    | 0.295±0.275 (N=5)             | 9070±3.25                                  | 9070 ( <i>A. vicina</i> )                                |
| Angular (rad s <sup>-2</sup> ) | 4.43±7.77 (N=5)               | 2.58×10 <sup>6</sup> ±1.04×10 <sup>6</sup> | 2.58×10 <sup>6</sup> ( <i>A. vicina</i> )                |
| Duration of strike (ms)        | 24.98±9.68 (N=9)              | 3.26±0.41                                  | 21.72 ( <i>L. maculata</i> )                             |
| Time of max. linear speed (ms) | 15.36±5.78 (N=5)              | 1.06±0.18                                  | 14.30 ( <i>L. maculata</i> )                             |

Speed and acceleration were measured at the distal end of the propodus. Values are means ± s.d. N, number of individuals.

*maculata* and brine shrimp that swam from a stationary pipette in the *A. vicina* experiments – could explain the kinematic differences observed between these two species. Relative to body size, *A. vicina*'s strikes spanned a wider range of distances than those of *L. maculata*; furthermore, *A. vicina*'s strike speed was correlated with the distance to the prey (Fig. 7). These results suggest that greater strike distances could yield greater speeds in *L. maculata*. However, *L. maculata* also struck slowly in the field; several long-duration, predatory strikes (>33 ms) were recorded. In addition, nearly all of the strikes in *A. vicina*, whether slow or fast, exhibited evidence of

spring loading (linear propodus motion prior to a strike and saddle compression/extension) whereas there was no evidence of spring loading in *L. maculata*.

The observations generated from comparisons of these two species raise interesting predictions about the effect of size on prey capture kinematics in stomatopods. One possible explanation for these results is that small individuals strike with higher speeds and use the elastic energy storage mechanism until a particular size threshold, at which point the long appendage can be driven effectively by direct muscle contractions alone or the underlying exoskeletal springs become too large and stiff to operate (Patek et al., 2013). One interesting next step would be to compare spring mechanics and kinematics across differently sized *L. maculata*,

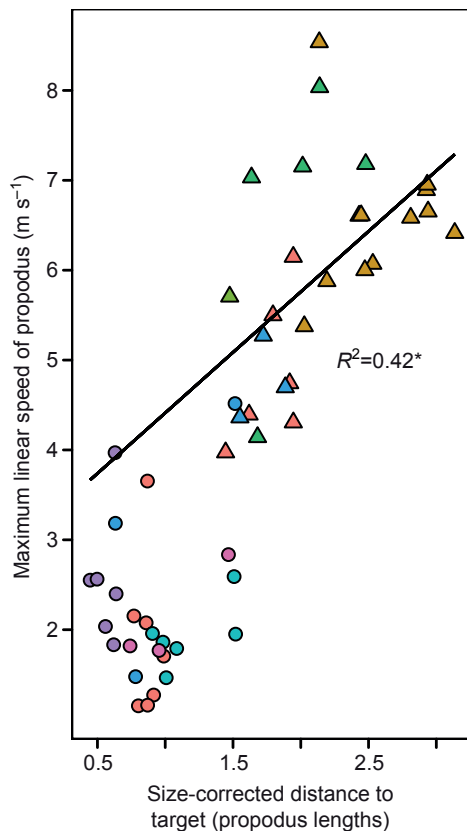


Fig. 7. Peak linear speed is positively correlated with the distance to prey in *A. vicina* (triangles), whereas *L. maculata* (circles) does not exhibit this association. The distance to target was size corrected by dividing this length by propodus length to account for body size differences between individuals. Each color represents a different individual and each point represents a different strike (*A. vicina*, \* $P=0.02$ ,  $F_{8,18}=3.28$ ,  $N=5$  individuals).

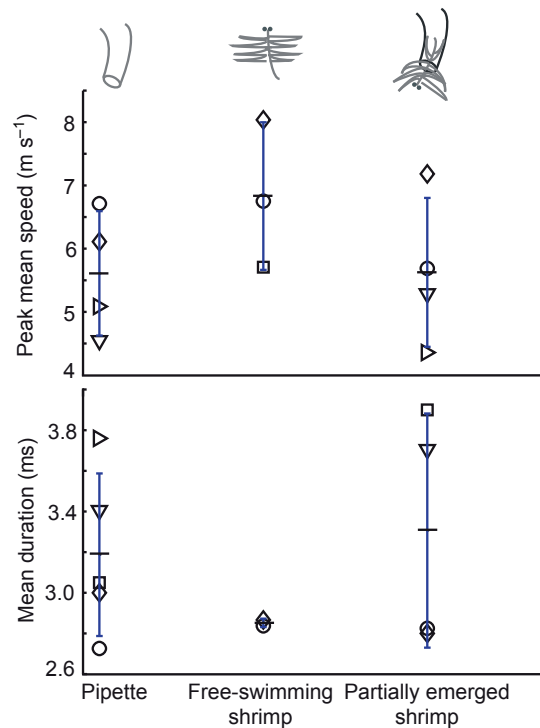


Fig. 8. Mean duration and mean peak linear speed of *A. vicina* during strikes at a pipette (left), freely swimming brine shrimp (middle) and brine shrimp emerging from the pipette (right). Each symbol is the mean of the peak values for a given individual. The horizontal lines show the mean of the individual means with error bars of ±1 s.d. The target did not have a significant effect on peak linear speed; however, target type did have a significant effect on strike duration, when examined along with effects of the individual and distance to the object.

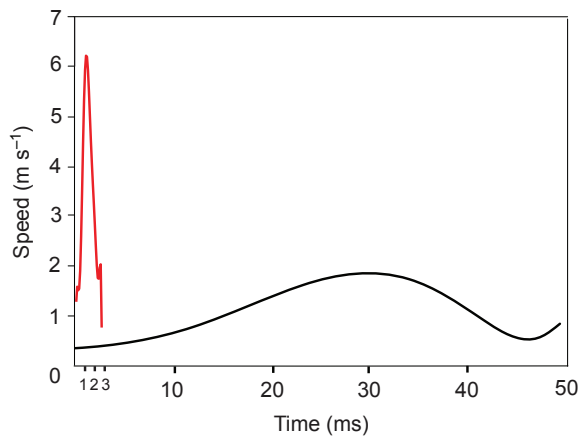


Fig. 9. *Alachosquilla vicina* (red line) strikes far more quickly and briefly than *L. maculata* (black line). Both profiles are representative strikes from each species and are derivatives of 10th order polynomial curve fits.

which range in total body length from 2 to 40 cm (Ahyong, 2001), to test these ideas.

#### Differences between spearsers and other mantis shrimp species

Smashing mantis shrimp have much higher strike speeds ( $10\text{--}23\text{ m s}^{-1}$ ) than the fastest spearsers ( $5.72\pm 0.91\text{ m s}^{-1}$ ). With undifferentiated dactyls, *Hemisquilla californiensis* (Hemisquillidae) crush and dislodge hard-shelled prey at  $10\text{ m s}^{-1}$  (Burrows, 1969). *Odontodactylus scyllarus* smash hard-shelled prey at  $14\text{--}23\text{ m s}^{-1}$  using hammer-shaped dactyls. The total body length of the *O. scyllarus* and *H. californiensis* individuals used in previous studies ranged from 11.5 to 14.8 cm (Patek et al., 2007) and from 25 to 30 cm (Burrows, 1969), respectively, which are about an order of magnitude greater than the largest *A. vicina* specimens used in this study, but are similar in size to *L. maculata*. Given that these large smashing species visibly use their elastic mechanism, one would have expected *L. maculata* to also use an elastic mechanism. This observation suggests that *L. maculata*'s size is not limiting its ability to generate spring-loaded strikes.

Spearsers strike with elongated, open dactyls, while smashers and generalized strikers that have undifferentiated appendages primarily hammer with highly calcified, massive dactyls that remain closed during the strike (Burrows, 1969; Caldwell and Dingle, 1976; Basch and Engle, 1989; Patek et al., 2004; Patek et al., 2007; Weaver et al., 2012). Spearer meral-Vs are narrow and curved (Fig. 4) compared with the robust, straight meral-Vs of smashers and undifferentiated species (Burrows, 1969; Patek et al., 2004; Patek et al., 2007). Similarly, spearer saddles are longer, narrower and more curved (Fig. 4) compared with the saddles of *H. californiensis* and *O. scyllarus* (Burrows, 1969; Patek et al., 2004; Patek et al., 2007). The mechanical and hydrodynamic consequences of these differences are not yet known, but new mathematical models of the smasher strike allow for future analyses of the effects of elastic energy storage, moment of inertia, mass and fluid dynamics on strike kinematics in spearsers (McHenry et al., 2012).

#### The behavior and kinematics of ambush predation

In the field, *L. maculata* captured prey primarily at night. A large portion of their time was spent scanning the environment for visual and chemosensory cues as evidenced by eye rotation and antennule flicking (Mead, 2002). Once an individual detected prey, it rapidly

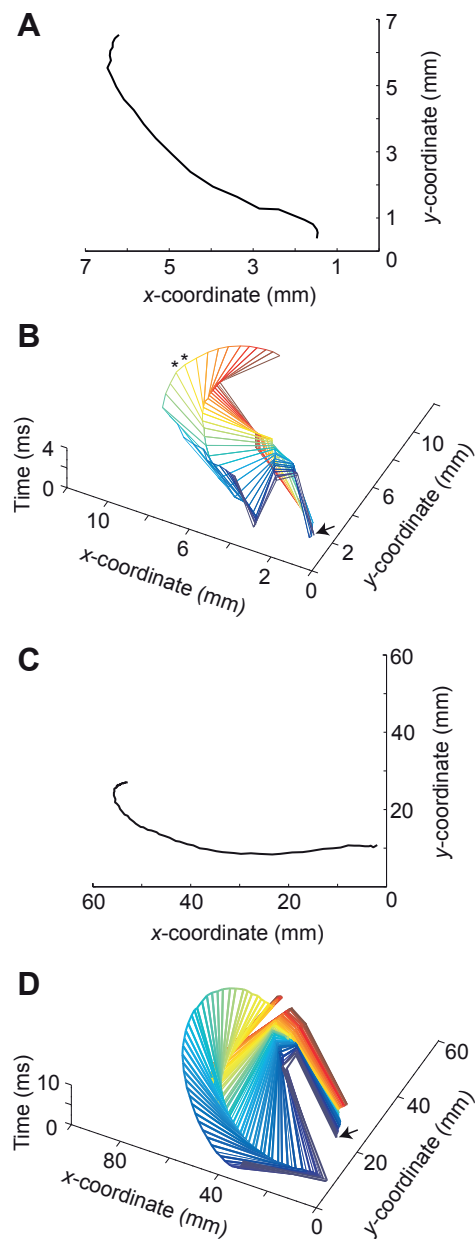


Fig. 10. Comparison of *A. vicina* (A,B) and *L. maculata* (C,D) strike kinematics. (A,C) The trajectory of the distal tip of the propodus for a typical strike through two spatial dimensions; (B,D) the entire appendage as it moves through time, where time increments between each line segment are 0.1 and 0.3 ms, respectively. Lines were drawn from the proximal to distal end of each appendage segment so that each segment is represented as a line. The different colors represent the changing positions of each segment through time, with time beginning at the purple line (and the arrows) and ending at the brown line. The x-axis represents lateral movement of the appendage and is oriented from the proximal to distal ends of the appendage, while the y-axis represents the vertical movement of the appendage and shows the position of the appendage relative to the anterior–posterior axis of the animal. The arrows represent the base of the merus at time zero in both species. We were unable to digitize the tip of the dactyl at the two points indicated by asterisks in B; these points were added in by hand to enhance visualization of the strike.

lunged from its burrow, opened the dactyl and struck in less than 66 ms ( $<1\text{--}2$  video frames). Thus, field and laboratory prey-capture behaviors were similar.

Considering ambush predation more broadly, the kinematics are as much about the escape response of the prey as the speed of the predator. Thus, one would predict that ambush predators should require strikes of the greatest speed and shortest duration to give an element of surprise, compared with foragers of sedentary prey which should not need strikes of high speed and short duration (Cooper et al., 1985; Viladiu et al., 1999; Webb, 1984; Wilga et al., 2007). Support for this prediction is provided by several groups of small aquatic ambush predators, such as odonate larvae, hemipterans and juvenile guppies (*Gambusia affinis*). The ambush predators that consume evasive, fast-moving plankton strike with higher accelerations compared with closely related species that forage for sedentary planktonic prey (Cooper et al., 1985).

Our study and review of the literature, however, cast doubt on the universality of the predictions described above. Actively foraging smashers strike with far higher speeds than spearers. In fact, the basal species *H. californiensis*, which has an undifferentiated appendage, also produces considerably faster appendage strikes of  $10\text{ m s}^{-1}$  (Ahyong, 2001; Ahyong and Jarman, 2009; Burrows, 1969). Thus, in mantis shrimp, the extreme predatory strikes documented in smashers may result from a need to produce high accelerations and maximize strike force, rather than the more traditional assumption that high speeds are for capturing fast prey (McHenry et al., 2012; Patek and Caldwell, 2005).

Perhaps even more interesting is the finding that the average duration of propodus rotation in *L. maculata* is comparable to the strike durations of both ambush and pursuit predators. The piscivorous garter snake, *T. rufipunctatus*, an ambush predator, achieves peak mouth-opening speeds of  $0.82\text{ m s}^{-1}$  in  $\sim 30\text{--}35\text{ ms}$  (Alfaro, 2002) and another ambush predator, a suction-feeding wrasse, *S. cabrilla*, has an average time to peak gape of 43 ms (Viladiu et al., 1999). Teleosts such as the largemouth bass, blue gill sunfish, midas cichlids and eels reach peak gape in  $\sim 22\text{--}38\text{ ms}$  (deVries and Wainwright, 2006; Higham et al., 2006), 32 ms (Higham et al., 2005), 30 ms (Mehta and Wainwright, 2007) and even 347 ms (Mehta and Wainwright, 2007), respectively. *Lysiosquillina maculata*'s strike durations are also similar to the protraction of squid tentacles, which occurs in 20–50 ms (reviewed in van Leeuwen et al., 2000). Unlike *L. maculata*, these aquatic predators swim toward their prey (Higham et al., 2005); however, some of the durations listed above were collected from predators that successfully captured their prey while the predators were stationary (Higham et al., 2005; Mehta and Wainwright, 2007). Thus, as long as ambush and pursuit predators reach their prey, ideally before the prey fully accelerates, they may only need to attain minimal speeds and accelerations.

Empirical studies in terrestrial lizards and birds, which compare ambush to active predatory kinematics, support the idea that ambush predators may not need to produce extremely fast speeds to successfully capture prey (Huey and Pianka, 1981; Eckhardt, 1979). Desert lacertid lizards that ambush mobile coleopteran prey exhibit slower mean running velocities compared with actively foraging lizards, which consume relatively sedentary termite prey (Huey and Pianka, 1981). Simulation studies modeling the success of ambush versus active predation as a function of prey velocity and predator strike velocity further show that when predators do not move as fast as their prey, the ambush strategy yields greater capture success, because encounter rates with prey are greater compared with the active-foraging strategy (Scharf et al., 2006; Avgar et al., 2008; Scharf et al., 2008).

The combined observations that (1) the larger *L. maculata* moves more slowly than the tiny *A. vicina*, (2) both *L. maculata* and *A.*

*vicina* fully extend long appendages, yielding slower strikes than smashing mantis shrimp species, and (3) other aquatic predators of evasive prey operate at similar speeds to *L. maculata*, suggest trade-offs between reach, accuracy and speed in aquatic ambush predators. Specifically, an aquatic ambush predator must overcome the challenges of rapidly traversing a potentially large distance between the hiding place and the prey while also striking accurately over short time scales. For example, the large, slow *L. maculata* has a long reach that permits acquisition of unsuspecting prey at great distances, and their use of direct muscle control rather than a pre-loaded elastic system may permit greater accuracy and control during the strike. Decreasing the speed and acceleration of prey capture in some fish predators has been shown to increase accuracy, because the predator has more time to adjust its alignment towards the prey before making contact (Higham, 2007). Likewise, small individuals with short appendages, such as *A. vicina*, have a smaller striking range and an increased chance of contacting their prey, and, therefore, can strike at greater speeds without incurring a loss of accuracy. Future studies considering the combined roles of kinematics, energetics and prey escape behavior will hopefully begin to reveal the proximate and evolutionary factors leading to these distinct prey-capture strategies.

#### ACKNOWLEDGEMENTS

We are especially grateful to R. Caldwell for animal acquisition and for thoughtful discussion on this manuscript. We thank R. Tigue for assistance with kinematic data collection, T. Claverie and E. Staaterman for field assistance, C. Huffard for illustrations, and S. Beissinger, T. Claverie, T. Dawson, R. Dudley, M. Rosario, E. Staaterman, J. Taylor, T. Tunstall and P. Wainwright for help with data analysis and for insightful comments on the manuscript. Micro-CT scans and analyses were performed at the Center for Nanoscale Systems at Harvard University, a member of the National Nanotechnology Infrastructure Network (National Science Foundation award no. ECS-0335765) and the High-Resolution X-ray Computed Tomography Facility of the University of Texas at Austin.

#### FUNDING

This research was funded by the Radcliffe Institute for Advanced Studies (SNP), a National Science Foundation Integrative Organismal Systems grant (no. 1014573 to S.N.P.) and the Department of Integrative Biology Gray Endowment Research Fellowship and Summer Research Fellowship (M.S.d.V.).

#### REFERENCES

- Ahyong, S. (2001). Revision of the Australian stomatopod Crustacea. *Rec. Aust. Mus.* **26**, 1-326.
- Ahyong, S. and Jarman, S. (2009). Stomatopod interrelationships: preliminary results based on analysis of three molecular loci. *Arthropod Syst. Phylogen.* **67**, 91-98.
- Alfaro, M. E. (2002). Forward attack modes of aquatic feeding garter snakes. *Funct. Ecol.* **16**, 204-215.
- Avgar, T., Horvitz, N., Broitman, L. and Nathan, R. (2008). How movement properties affect prey encounter rates of ambush versus active predators: a comment on Scharf et al. *Am. Nat.* **172**, 593-595.
- Bailey, P. C. E. (1986). The feeding behavior of a sit-and-wait predator, *Fanatra dispar*, (Heteroptera: Nepidae): description of behavioral components of prey capture, and the effect of food deprivation on predator arousal and capture dynamics. *Behaviour* **97**, 66-93.
- Basch, L. V. and Engle, J. M. (1989). Aspects of the ecology and behavior of the stomatopod *Hemisquilla ensigera californiensis* (Gonodactyloidea: Hemisquillidae). In *Biology of Stomatopods: Proceedings of the 1st International Workshop on Stomatopod Biology* (ed. E. A. Ferrero), pp. 199-212. Modena: Mucchi.
- Bilcke, J., Herrel, A. and Van Damme, R. (2006). Correlated evolution of aquatic prey-capture strategies in European and American naticine snakes. *Biol. J. Linn. Soc. Lond.* **88**, 73-83.
- Burrows, M. (1969). The mechanics and neural control of the prey capture strike in the mantid shrimps *Squilla* and *Hemisquilla*. *J. Comp. Physiol.* **A 62**, 361-381.
- Burrows, M. and Hoyle, G. (1972). Neuromuscular physiology of the strike mechanism of the mantis shrimp, *Hemisquilla*. *J. Exp. Zool.* **179**, 379-394.
- Caldwell, R. L. (1991). Variation in reproductive behavior in stomatopod Crustacea. In *Crustacean Sexual Biology* (ed. R. Bauer and J. Martin), pp. 67-90. New York: Columbia University Press.
- Caldwell, R. L. and Dingle, H. (1975). Ecology and evolution of agonistic behavior in stomatopods. *Naturwissenschaften* **62**, 214-222.
- Caldwell, R. L. and Dingle, H. (1976). Stomatopods. *Sci. Am.* **234**, 80-89.
- Casatti, L. and Castro, R. M. C. (2006). Testing the ecomorphological hypothesis in a headwater riffles fish assemblage of the Rio Sao Francisco, southeastern Brazil. *Neotrop. Ichthyol.* **4**, 203-214.

- Claverie, T., Chan, E. and Patek, S. N. (2011). Modularity and scaling in fast movements: power amplification in mantis shrimp. *Evolution* **65**, 443-461.
- Cooper, S. D., Smith, D. W. and Bence, J. R. (1985). Prey selection by freshwater predators with different foraging strategies. *Can. J. Fish. Aquat. Sci.* **42**, 1720-1732.
- Corrette, B. J. (1990). Prey capture in the praying mantis *Tenodera aridifolia sinensis*: coordination of the capture sequence and strike movements. *J. Exp. Biol.* **148**, 147-180.
- Daniels, R. A. (1982). Feeding ecology of some fishes of the Antarctic Peninsula. *Fish Bull.* **80**, 575-588.
- Deban, S., O'Reilly, J. C. and Nishikawa, K. C. (2001). The evolution of the motor control of feeding in amphibians. *Am. Zool.* **41**, 1280-1298.
- deVries, M. S. and Wainwright, P. C. (2006). The effects of acute temperature change on prey capture kinematics in largemouth bass, *Micropterus salmoides*. *Copeia* **2006**, 437-444.
- Dingle, H. and Caldwell, R. L. (1978). Ecology and morphology of feeding and agonistic behavior in mudflat stomatopods (Squillaidae). *Biol. Bull.* **155**, 134-149.
- Eckhardt, R. C. (1979). The adaptive syndromes of two guilds of insectivorous birds in the Colorado Rocky Mountains. *Ecol. Monogr.* **49**, 129-149.
- Es skew, E. A., Willson, J. D. and Winne, C. T. (2009). Ambush site selection and ontogenetic shifts in foraging strategy in a semi-aquatic pit viper, the Eastern cottonmouth. *J. Zool.* **277**, 179-186.
- Formanowicz, D. R. and Brodie, E. D. (1988). Prey density and ambush site changes in the *Tropisternus lateralis* larvae (Coleoptera: Hydrophilidae). *J. Kans. Entomol. Soc.* **61**, 420-427.
- Garland, T., Jr and Adolph, S. C. (1994). Why not to do two-species comparative studies: limitations on inferring adaptation. *Physiol. Zool.* **67**, 797-828.
- Garland, T., Jr and Losos, J. B. (1994). Ecological morphology of locomotor performance in squamate reptiles. In *Ecological Morphology: An Integrative Approach to Organismal Biology* (ed. P. C. Wainwright), pp. 240-302. Chicago, IL: University of Chicago Press.
- Greef, J. M. and Whiting, M. F. (2000). Foraging-mode plasticity in the lizard *Platysaurus broadleyi*. *Herpetologica* **56**, 402-407.
- Hamano, T. and Matsuura, S. (1986). Optimal prey size for the Japanese mantis shrimp from structure of the raptorial claw. *Nippon Suisan Gakkai Shi* **52**, 1-10.
- Higham, T. E. (2007). The integration of locomotion and prey capture in vertebrates: morphology, behavior, and performance. *Integr. Comp. Biol.* **47**, 82-95.
- Higham, T. E., Day, S. W. and Wainwright, P. C. (2005). Sucking while swimming: evaluating the effects of ram speed on suction generation in bluegill sunfish *Lepomis macrochirus* using digital particle image velocimetry. *J. Exp. Biol.* **208**, 2653-2660.
- Higham, T. E., Day, S. W. and Wainwright, P. C. (2006). Multidimensional analysis of suction feeding performance in fishes: fluid speed, acceleration, strike accuracy and the ingested volume of water. *J. Exp. Biol.* **209**, 2713-2725.
- Huey, R. B. and Pianka, E. R. (1981). Ecological consequences of foraging mode. *Ecology* **62**, 991-999.
- Huey, R. B., Bennett, A. F., John-Alder, H. B. and Nagy, K. A. (1984). Locomotor capacity and foraging behavior of Kalahari lacertid lizards. *Anim. Behav.* **32**, 41-50.
- Hulbert, L. B., Sigler, M. F. and Lunsford, C. R. (2006). Depth and movement behavior of the Pacific sleeter shark in the north-east Pacific Ocean. *J. Fish Biol.* **69**, 406-425.
- Jiang, H. and Paffenhöfer, G.-A. (2008). Hydrodynamic signal perception by the copepod *Oithona plumifera*. *Mar. Ecol. Prog. Ser.* **373**, 37-52.
- Kiorboe, T., Jiang, H. and Colin, S. P. (2010). Danger of zooplankton feeding: the fluid signal generated by ambush-feeding copepods. *Proc. R. Soc. B* **277**, 3229-3237.
- Kral, K., Vernik, M. and Devetak, D. (2000). The visually controlled prey-capture behaviour of the European mantispid *Mantispa styriaca*. *J. Exp. Biol.* **203**, 2117-2123.
- McBrayer, L. D. and Wylie, J. E. (2009). Concordance between locomotor morphology and foraging mode in lacertid lizards. *Zoology* **112**, 370-378.
- McHenry, M. J., Claverie, T., Rosario, M. V. and Patek, S. N. (2012). Gearing for speed slows the predatory strike of a mantis shrimp. *J. Exp. Biol.* **215**, 1231-1245.
- McNeill, P., Burrows, M. and Hoyle, G. (1972). Fine structures of muscles controlling the strike of the mantis shrimp *Hemisquilla*. *J. Exp. Zool.* **179**, 395-416.
- Mead, K. S. (2002). From odor molecules to plume tracking: an interdisciplinary, multilevel approach to olfaction in stomatopods. *Integr. Comp. Biol.* **42**, 258-264.
- Mehta, R. S. and Wainwright, P. C. (2007). Biting releases constraints on moray eel feeding kinematics. *J. Exp. Biol.* **210**, 495-504.
- Miles, D. B., Losos, J. B. and Irschick, D. (2007). Morphology, performance, and foraging mode. In *Lizard Ecology: The Evolutionary Consequences of Foraging Mode* (ed. S. M. Reilly, L. D. McBrayer and D. B. Miles), pp. 49-93. Cambridge, UK: Cambridge University Press.
- Ostrand, K. G., Braeutigam, B. J. and Wahl, D. H. (2004). Consequences of vegetation density and prey species on spotted gar foraging. *Trans. Am. Fish. Soc.* **133**, 794-800.
- Patek, S. N. and Caldwell, R. L. (2005). Extreme impact and cavitation forces of a biological hammer: strike forces of the peacock mantis shrimp *Odontodactylus scyllarus*. *J. Exp. Biol.* **208**, 3655-3664.
- Patek, S. N., Korff, W. L. and Caldwell, R. L. (2004). Biomechanics: deadly strike mechanism of a mantis shrimp. *Nature* **428**, 819-820.
- Patek, S. N., Nowroozi, B. N., Baio, J. E., Caldwell, R. L. and Summers, A. P. (2007). Linkage mechanics and power amplification of the mantis shrimp's strike. *J. Exp. Biol.* **210**, 3677-3688.
- Patek, S. N., Dudek, D. M. and Rosario, M. V. (2011). From bouncy legs to poisoned arrows: elastic movements in invertebrates. *J. Exp. Biol.* **214**, 1973-1980.
- Patek, S. N., Rosario, M. V. and Taylor, J. R. A. (2013). Comparative spring mechanics in mantis shrimp. *J. Exp. Biol.* (in press).
- Pianka, E. R. (1966). Convexity, desert lizards, and spatial heterogeneity. *Ecology* **47**, 1055-1059.
- Porter, M. L., Zhang, Y., Desai, S., Caldwell, R. L. and Cronin, T. W. (2010). Evolution of anatomical and physiological specialization in the compound eyes of stomatopod crustaceans. *J. Exp. Biol.* **213**, 3473-3486.
- Riechert, S. E. and Luczak, J. (1982). Spider foraging: behavioral responses to prey. In *Spider Communication: Mechanisms and Ecological Significance* (ed. P. N. Witt and J. Rovner), pp. 353-385. Princeton, NJ: Princeton University Press.
- Sano, K. and Kurokura, H. (2011). Predatory behavior of the backswimmer (*Anisops ogasawarensis*). *Aquaculture* **317**, 210-213.
- Scharf, I., Nulman, E., Ovadia, O. and Bouskila, A. (2006). Efficiency evaluation of two competing foraging modes under different conditions. *Am. Nat.* **168**, 350-357.
- Scharf, I., Ovadia, O. and Bouskila, A. (2008). Prey encounter rate by predators: discussing the realism of grid-based models and how to model the predator's foraging mode: a reply to Avgar et al. *Am. Nat.* **172**, 596-598.
- van Leeuwen, J. L., De Groot, J. H. and Kier, W. M. (2000). Evolutionary mechanics of protrusible tentacles and tongues. *Neth. J. Zool.* **50**, 113-139.
- Viladiu, C., Vandewalle, P., Osse, J. W. M. and Casinos, A. (1999). Suction feeding strategies of two species of Mediterranean Serranidae (*Serranus cabrilla* and *Serranus scriba*). *Neth. J. Zool.* **49**, 81-95.
- Walker, J. A. (1998). Estimating velocities and accelerations of animal locomotion: a simulation experiment comparing numerical differentiation algorithms. *J. Exp. Biol.* **201**, 981-995.
- Weaver, J. C., Milliron, G. W., Miserez, A., Evans-Lutterodt, K., Herrera, S., Gallana, I., Mershon, W. J., Swanson, B., Zavattieri, P., DiMasi, E. et al. (2012). The stomatopod dactyl club: a formidable damage-tolerant biological hammer. *Science* **336**, 1275-1280.
- Webb, P. W. (1984). Body form locomotion and foraging in aquatic vertebrates. *Am. Zool.* **24**, 107-120.
- Wilga, C. D., Motta, P. J. and Sanford, C. P. (2007). Evolution and ecology of feeding in elasmobranchs. *Integr. Comp. Biol.* **47**, 55-69.
- Zack, T. I., Claverie, T. and Patek, S. N. (2009). Elastic energy storage in the mantis shrimp's fast predatory strike. *J. Exp. Biol.* **212**, 4002-4009.